Supporting Information

Hierarchical Porous Carbon Microspheres with Superhydrophilic Surface for Efficient Adsorption and Detection of Water-Soluble Contaminants

Junfang Li, Hua Bai, Wei Liu, Xinshi Li, Wentao Li, Junfeng Zhai, Mengchen Li, and Guangcheng Xi*

Institute of Industrial and Consumer Product Safety, Chinese Academy of Inspection and Quarantine, Beijing 100176, P. R. China.

Corresponding authors: xiguangcheng@caiq.gov.cn

Experimental Section

Enhanced Factor Calculation

To calculate the EF of the Au/NCMS, the ratio of SERS to normal Raman spectra (NRS) of R6G was determined by using the following calculating formula 1

$$EF = (I_{SERS}/N_{SERS})/(I_{NRS}/N_{NRS}) \quad (1)$$

$$N_{SERS} = N_A n S_{Irr}/S_{dif} \quad (2)$$

$$N_{NRS} = d S_{Irr} h N_A/M \quad (3)$$

where I_{SERS} and I_{NRS} refer to the peak intensities of the SERS and NRS, respectively. N_{SERS} and N_{NRS} correspond to the number of probe molecules excited in the SERS and NRS tests. In the SERS measurements, Raman scattering peak, R_1 at 612 cm^{-3} was selected for the calculations of the EF. For comparison, the peak intensities of the R6G (10^{-9}, 10^{-11}, 10^{-13} M, aqueous solution) directly placed on bare glass were detected as NRS data. To decrease the measuring error, the intensities were obtained by continually ran the test procedure at randomly selected 50 points and took the average. N_{SERS} is

calculated by formula 2, where N_A refer to the Avogadro's constant, n correspond to the molar quantity of the probe molecule, S_{Irr} refer to the irradiation area under the laser beam (5 μm in diameter), and S_{dif} refer to the diffusion area of the substance to be tested on the substrate. In a typical test, one drop (20 microliter) of the probe solution was dropped onto the SERS substrate, and the probe solution was spread into a circle with a diameter of 4 mm when the solution is completely dry. N_{NRS} is determined by the formula 3, where d is the packing density of R6G molecules in the surface of substrate (1.4×10^{21} molecule/cm^3), h refer to the laser confocal depth (26 μm), M correspond to the molecule weight of R6G (479).

Figures

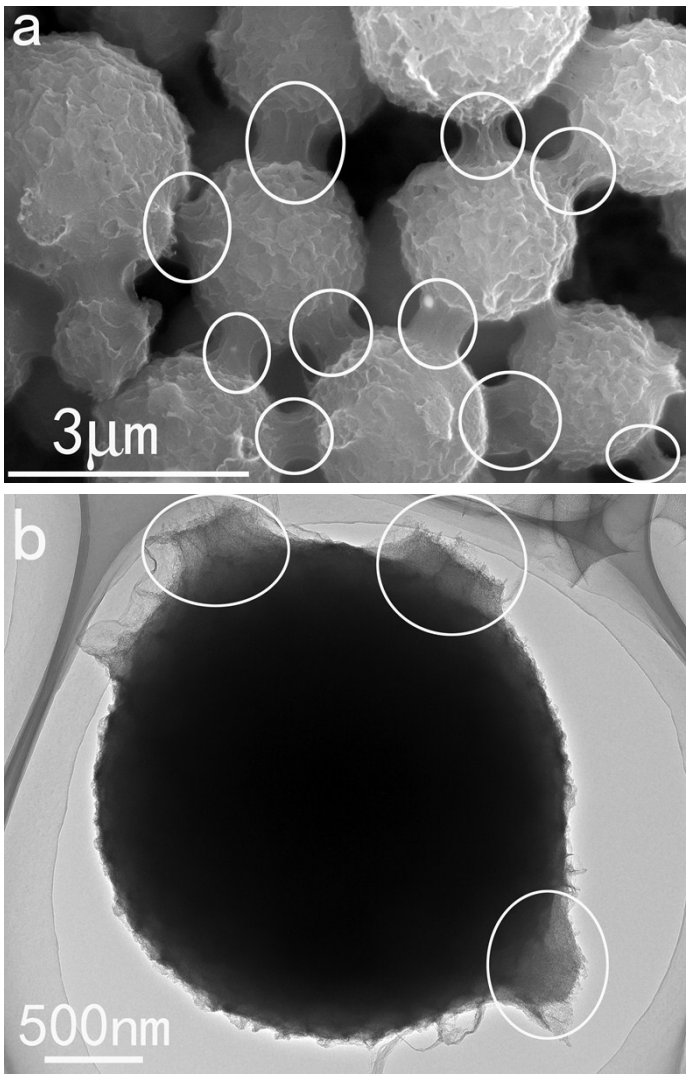

Figure S1.The morphology of the freeze-dried pomelo peel. (**a)** SEM image. (**b)** TEM image. The images show that pomelo peel contains a lot of interconnected networks of spherical particles. The connections between the sphere and the sphere can be seen clearly (marker with white circles).

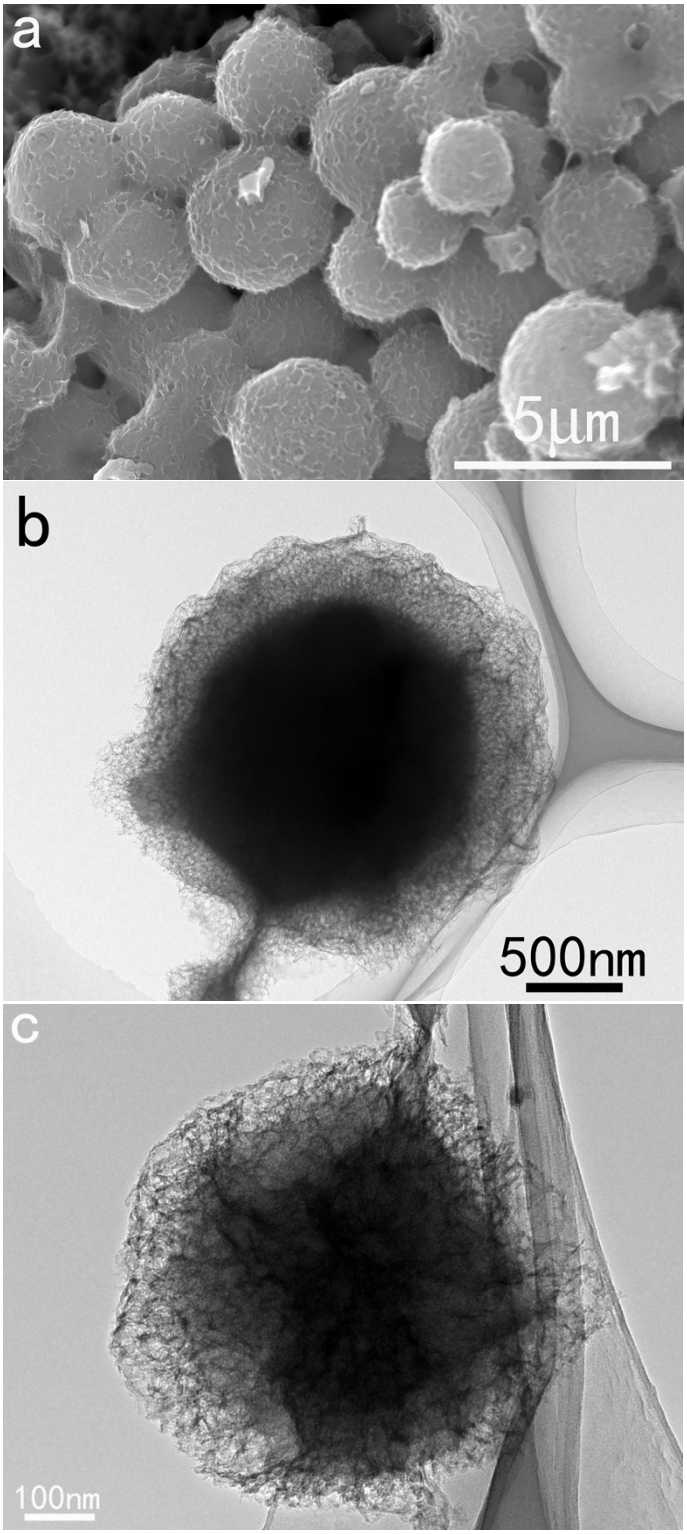

Figure S2. The SEM and TEM images of the HTC obtained after 2 h (**a-b**) and 8 h (**c**) hydrothermal treating.

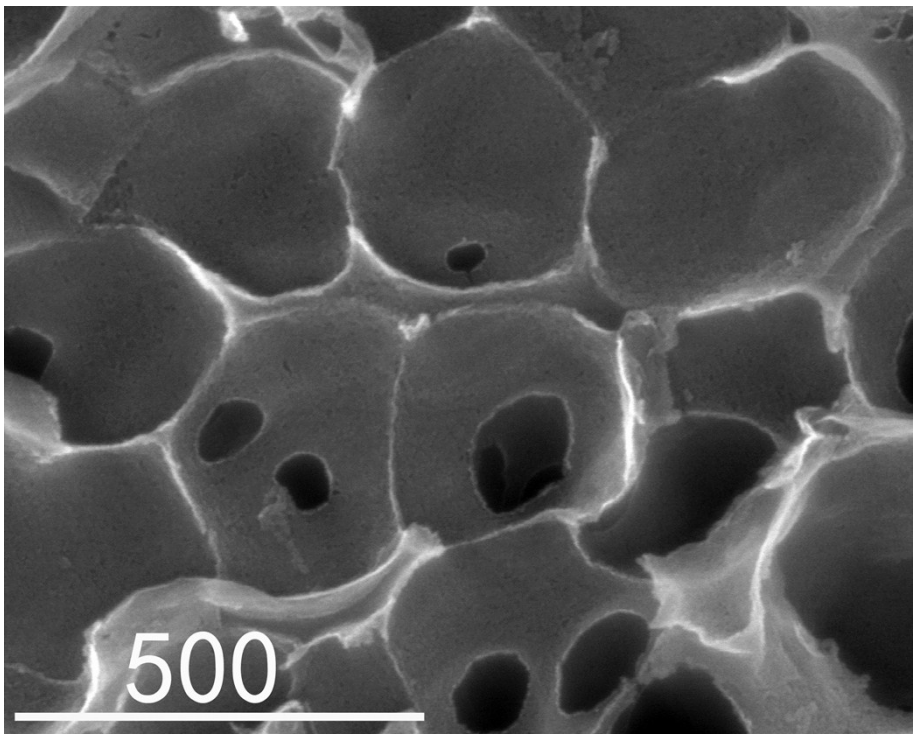

Figure S3. A high-magnification SEM image of the as-synthesized NCMS. From the image, it can be seen that many small pores are in the sheets.

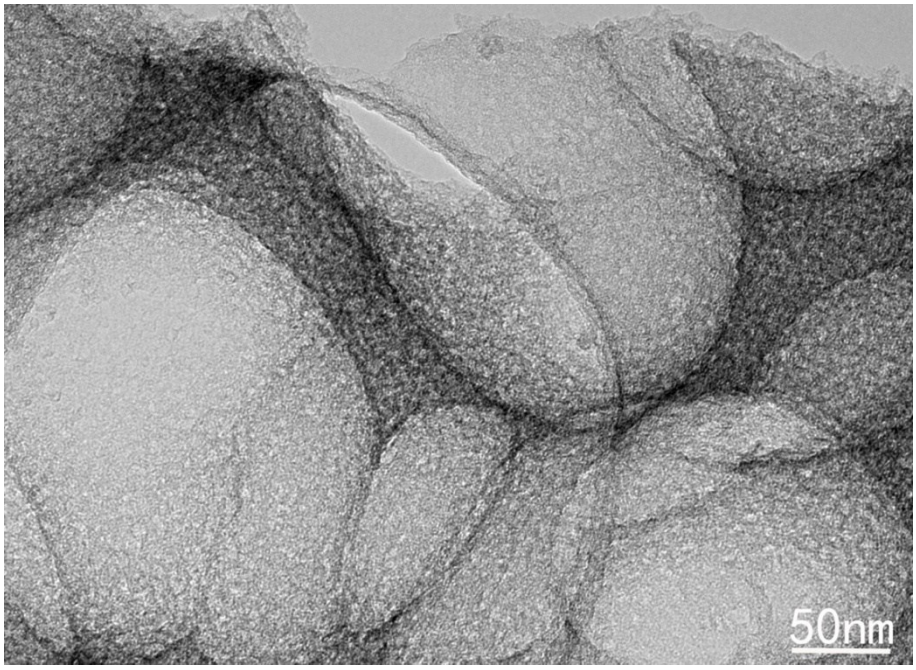

Figure S4. A high-magnification TEM image of the as-synthesized NCMS. From the image, it also can be seen that many small pores are in the sheets.

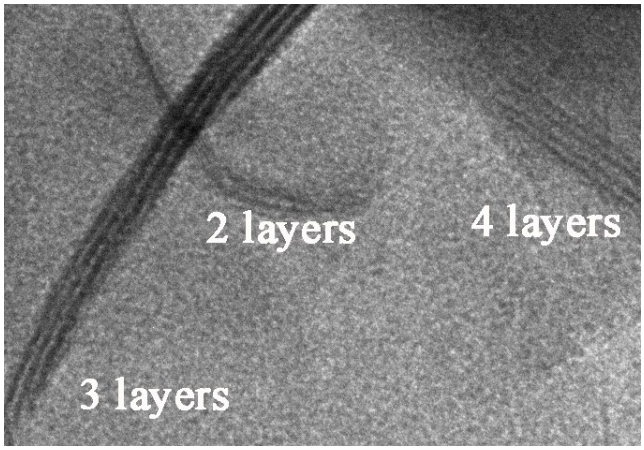

Figure S5. HRTEM image demonstrates that the graphene-like nanosheets, which shows that the layers of these carbon sheets are widely distributed, with 2 layers, 3 layers, and 4 layers.

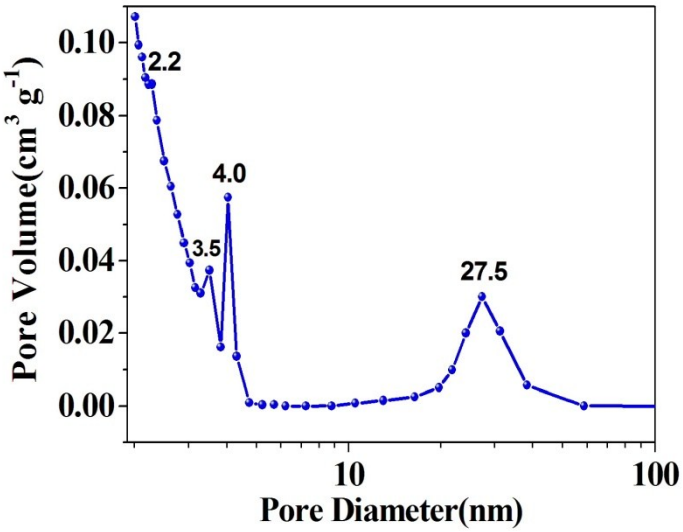

Figure S6. The Pore size distribution of the NCMS, which clearly indicates that the sample contains both mesopores (2-50 nm) and macropores (> 50 nm).

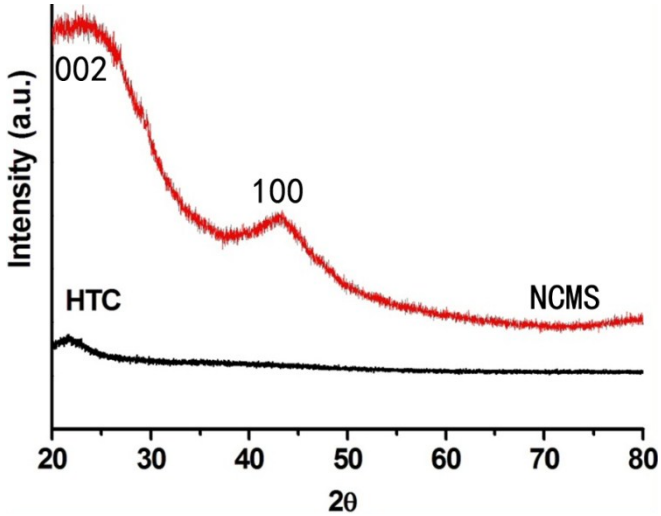

Figure S7. XRD patterns of the NCMS and HTC, which shown that NCMS contains ultrathin carbon sheets.

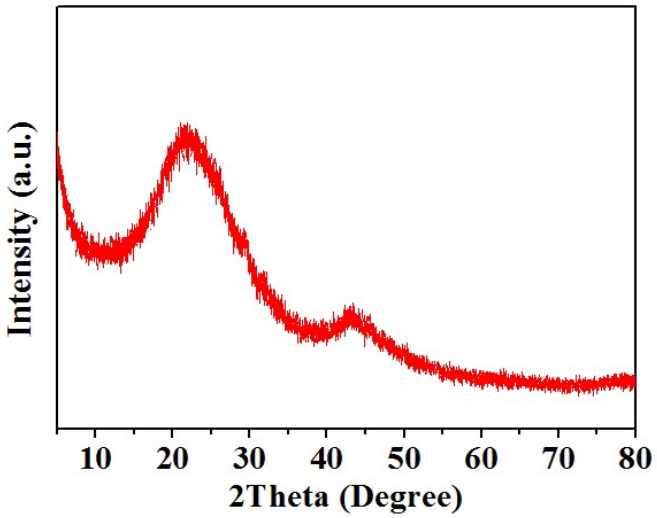

Figure S8. XRD patterns of the NCMS with wider range.

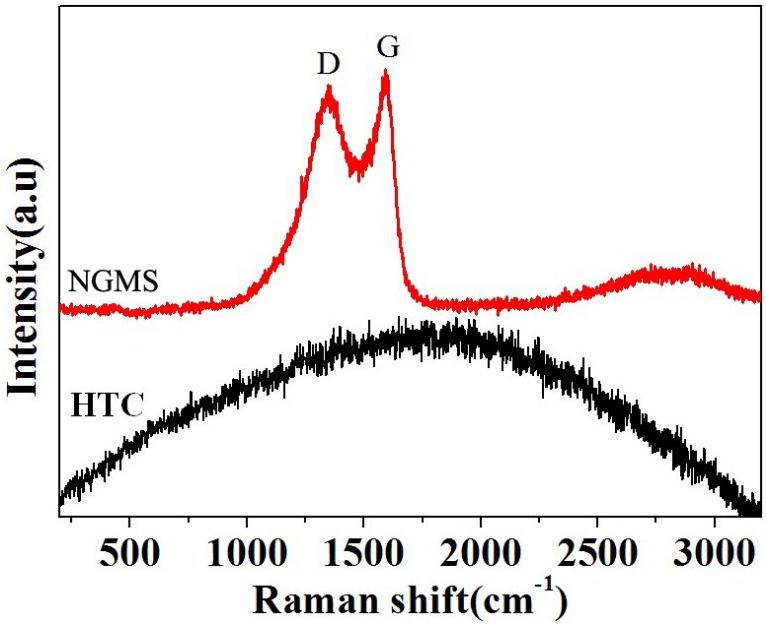

Figure S9. The Raman spectra of the HTC and NCMS.

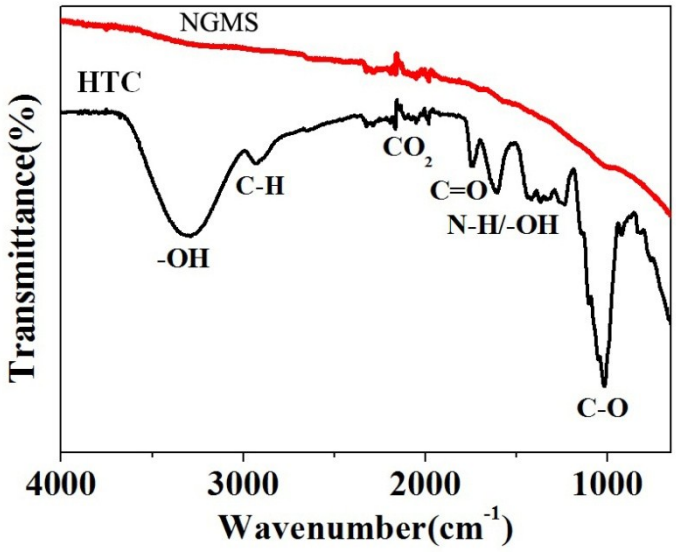

Figure S10. The FTIR spectra of the HTC and NCMS.

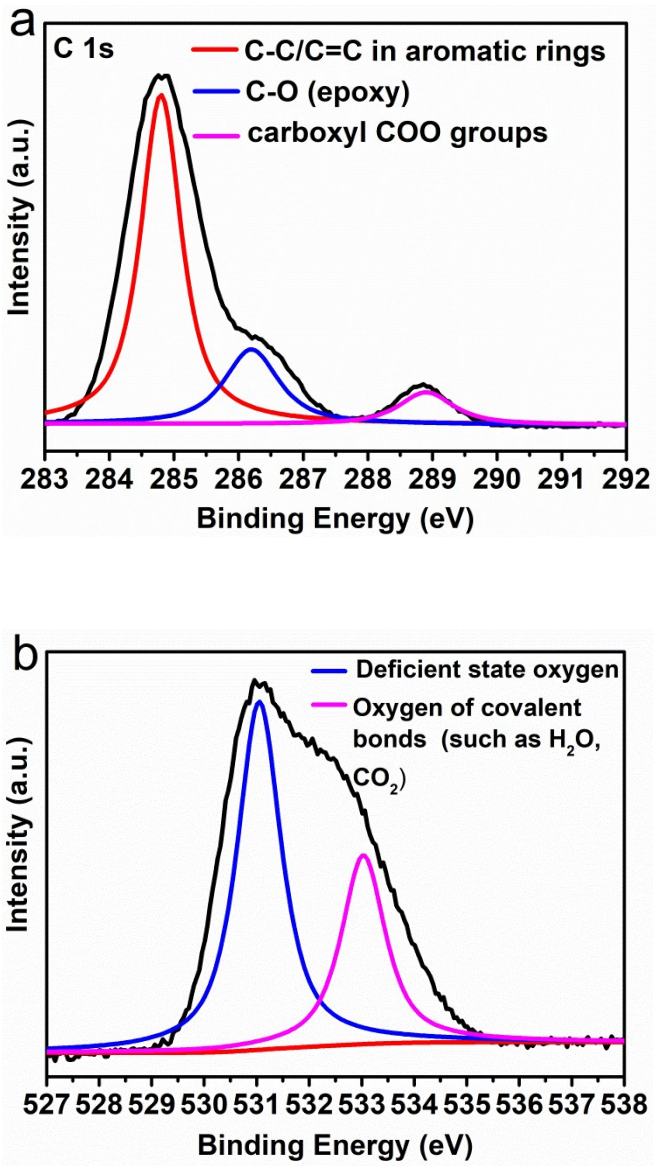

Figure S11. XPS spectrum of the C 1s and O 1s of the NCMS.

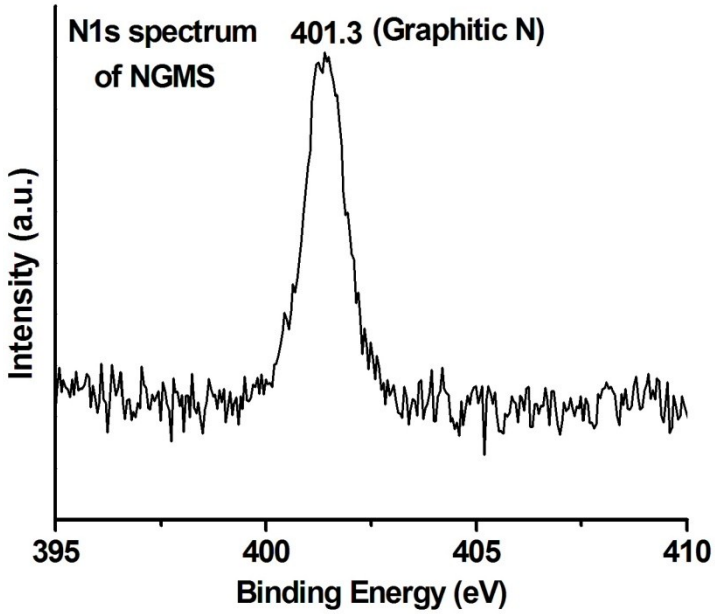

Figure S12. XPS spectrum of the N1s of the NCMS, which demonstrated that the N-atoms are graphitic N.

Figure S13. The density of HTC is about 1.5 mg cm^{-3}, which can stand firmly on the top of the very soft feathers.

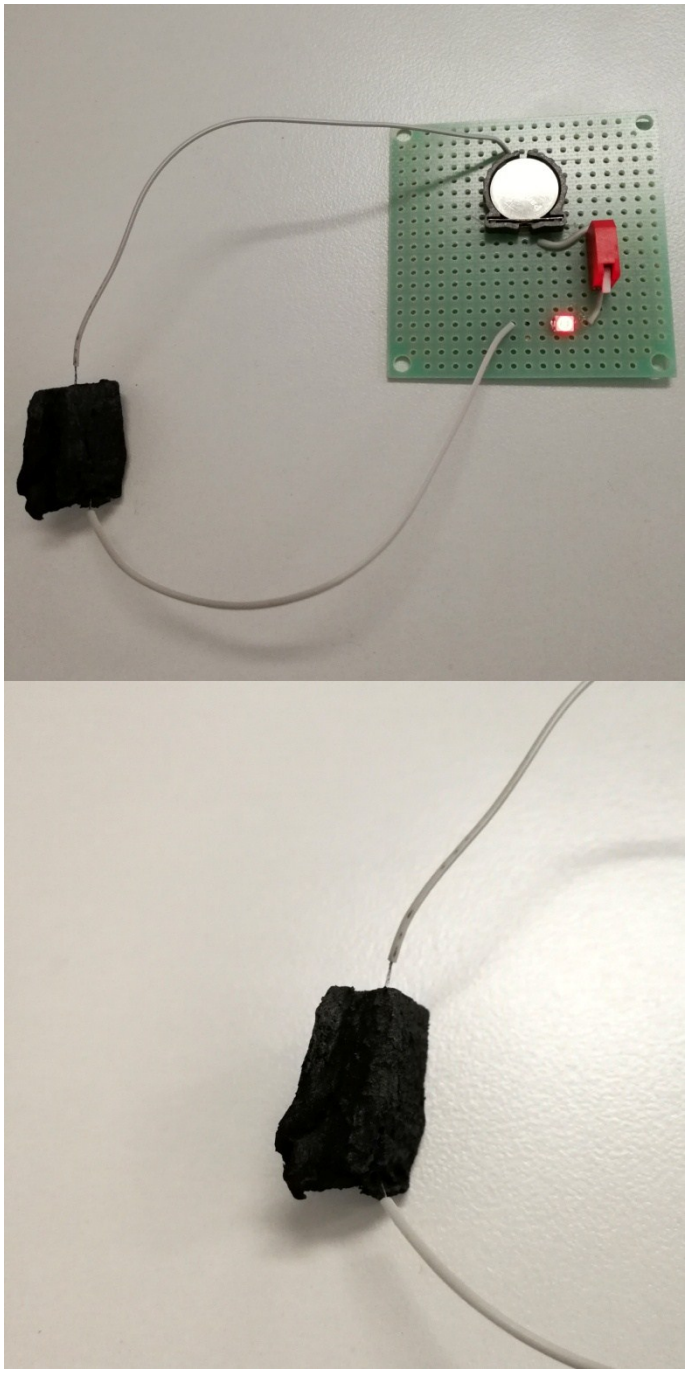

Figure S14. The conductivity of the NCMS is about 5×10^2 S m^{-1}. At 1.8 V, the current passes through the NCMS can make a red LED (I = 1.2 mA) give off light.

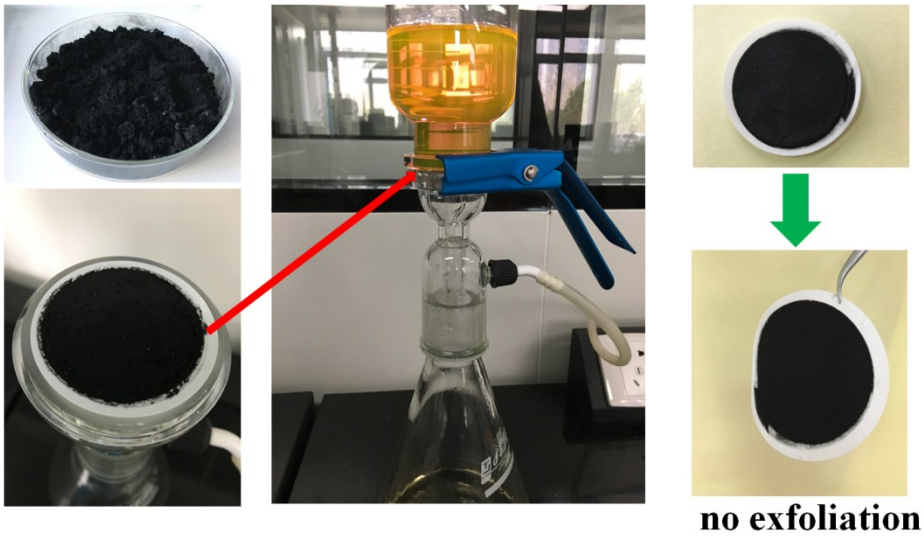

Figure S15. Device for adsorption experiments. The ground NCMS formed a filter layer in the mixed cellulose ester film through filtration. The filter layer is very stable, and even if the membrane is upright, the particles will not fall off.

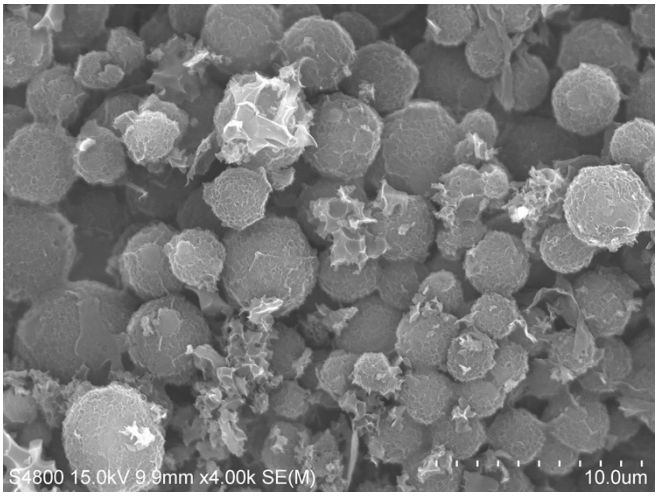

Figure S16. SEM image of the the ground NCMS.

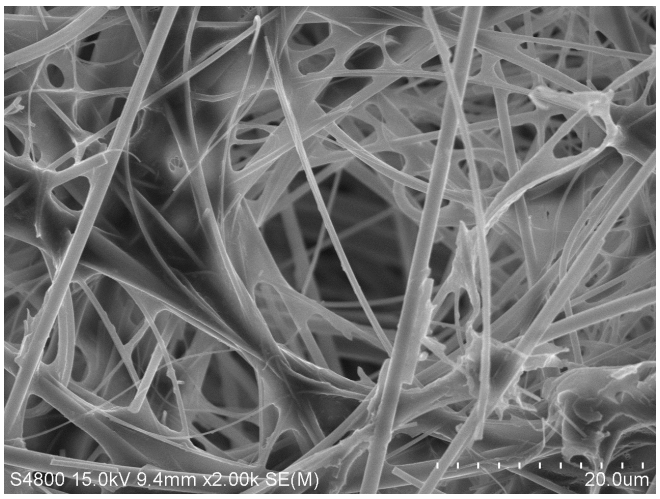

Figure S17. SEM image of the mixed cellulose filter membrane used in the adsorption experiments.

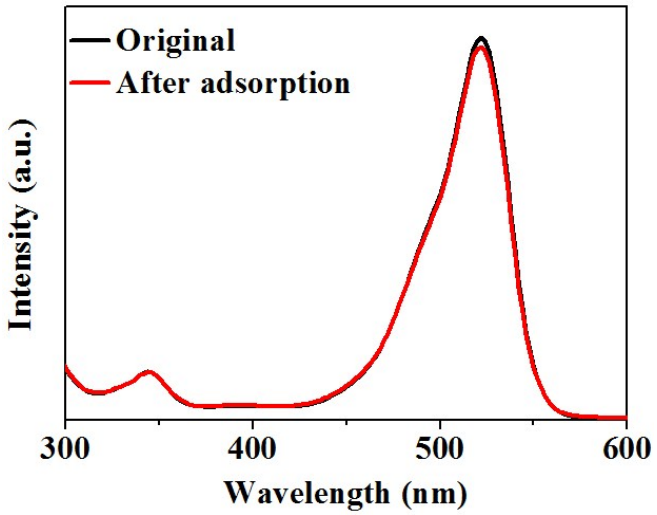

Figure S18. The adsorption of Rh6G by the mixed cellulose filter membrane did not change much, indicating that the adsorption of dye molecules on the membrane itself was not strong.

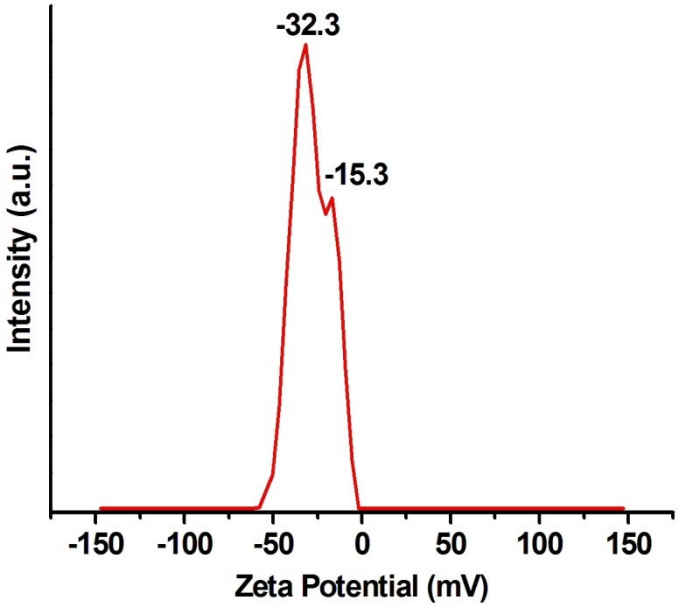

Figure S19. Zeta-potential analysis of the NCMS shown that the surface charge of the NCMS is negative, and the range of zeta-potential is -(15.3-32.3) mV.

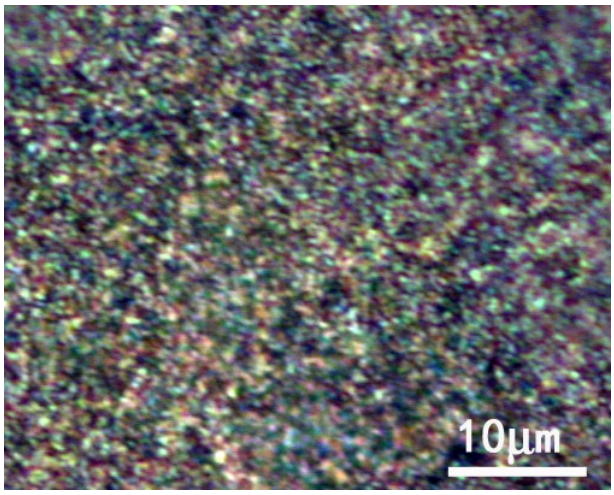

Figure S20. Optical photograph of the Au/NCMS substrate.

Table S1: Some of the Previously Reported Specific Surface Areas (BET) for Graphene-based Materials

Material	Composition	BET Area ($m^2 g^{-1}$)	Author
Pristine Graphene Aerogels	Graphene	**700**	Lin et al.[1]
Graphene Nanoribbon Aerogels	Graphene	**113**	Peng et al.[2]
Tubular Graphene	Graphene	**970**	Bi et al.[3]
N and B Co-doped Graphene	Graphene	**249**	Wu et al.[4]
Graphene Bulks	Graphene	**508**	Cheng et al.[5]
N-doped Graphene Networks	Graphene	**583**	Zhang et al.[6]
N-doped Graphene Foam	Graphene	**346**	Xu et al.[7]
Graphene Aerogel	Graphene	**463**	Ye et al.[8]
Ice-Templated N- Graphene	Graphene	**190**	Kota et al.[9]
Graphene Aerogel Fibers	Graphene	**884**	Xu et al.[10]
Porous Graphene Networks	Graphene	**1810**	Li et al.[11]
Interconnected Graphene Aerogel	Graphene	**850**	Chen et. al.[12]
Graphene Aerogel	Graphene	**512**	Zhang et. al.[13]
Graphene Tapes	Graphene	**400**	Korkut et. al.[14]
NCMS	**Porous Graphene**	**2850.4**	**This work**

References

[1] Y. Lin, F. Liu, G. Casano, R. Bhavsar, I. A. Kinloch, B. Derby, *Adv. Mater*. **2016**, *28*, 7993–8000.

[2] Q. Y. Peng, Y. B. Li, X. D. He, X. C. Gui, Y. Y. Shang, C. H. Wang, C. Wang, W. Zhao, S. Y. Du, E. Z. Shi, P. X. Li, D. H. Wu, A. Y. Cao, *Adv. Mater.* **2014**, *26*, 3241–3247.

[3] H. Bi, I. W. Chen, T. Q. Lin, F. Q. Huang, *Adv. Mater.* **2015**, *27*, 5943–5949.

[4] Z. S. Wu, A. Winter, L. Chen, Y. Sun, A. Turchanin, X. L. Feng, K. Müllen, *Adv. Mater.* **2012**, *24*, 5130–5135.

[5] H. H. Cheng, M. H. Ye, F. Zhao, C. G. Hu, Y. Zhao, Y. Liang, N. Chen, S. Chen, L. Jiang, L. T. Qu, *Adv. Mater.* **2016**, *28*, 3305–3312.

[6] W. L. Zhang, C. Xu, C. Q. Ma, G. X. Li, Y. Z. Wang, K. Y. Zhang, F. Li, C. Liu, H. M. Cheng, Y. W. Du, N. J. Tang, W. C. Ren, *Adv. Mater.* **2017**, *29*, 1701677.

[7] J. T. Xu, M. Wang, N. P. Wickramaratne, M. Jaroniec, S. X. Dou, L. M. Dai, *Adv. Mater*. **2015**, *27*, 2042.

[8] S. B. Ye, J. C. Feng, P. Y. Wu, *ACS Appl. Mater. Interfaces* **2013**, *5*, 7122.

[9] M. Kota, X. Yu, S. Yeon, H. Cheong, H. S. Park, *J. Power Sources* **2016**, *303*, 372.

[10] Z. Xu, Y. Zhang, P. G. Li, C. Gao, *ACS Nano*, **2012**, *6*, 7103-7113.

[11] Y. Y. Li , Z. S. Li , P. K. Shen, *Adv. Mater.* **2013**, *25*, 2474-2480.

[12] Z. P. Chen, W. C. Ren, L. B. Gao, B. L. Liu, S. F. Pei, H. M. Cheng, *Nat. Mater.* **2011**, *10*, 424–428.

[13] X. T. Zhang, Z. Y. Sui, B. Xu, S. F. Yue, Y. J. Luo, W. C. Zhan, B. Liu, *J. Mater. Chem.* **2011**, *21*, 6449-6497.

[14] S. Korkut, J. D. Roy-Mayhew, D. M. Dabbs, D. L. Milius, I. A. Aksay, *ACS Nano* **2011**, *5*, 5214-5222.